Transp Porous Med (2016) 111:287–304
DOI 10.1007/s11242-015-0594-6

The Effect of Conducting Sidewalls on the Onset of Convection in a Porous Cavity

Syakila Ahmad[1,2] · **D. Andrew S. Rees**[2]

Received: 27 July 2015 / Accepted: 17 October 2015 / Published online: 30 October 2015

Abstract In this short paper we consider the effect of the presence of conducting sidewalls of finite thickness on the onset of convection in a two-dimensional porous cavity. Two cases are considered where the outer boundaries of the sidewalls are either perfectly insulating or perfectly conducting. A unified theory is presented which combines both these cases, and the stability properties of the overall system is found to undergo a full transition from that of the classical Darcy–Bénard problem to that of the degenerate system studied in detail by Rees and Tyvand (J Eng Math 49:181–193, 2004).

Keywords Porous media · Convection · Instability · Darcy–Bénard

List of symbols

A	Arbitrary constant
c	Conductivity ratio
d	Aspect ratio of the sidelayers
F	Reduced streamfunction perturbation
g	Gravity
G	Reduced temperature perturbation
h	Height of the layer
k	Conductivity of the porous layer
k_s	Conductivity of the sidelayers
K	Permeability
L	Aspect ratio of the porous layer

✉ D. Andrew S. Rees
D.A.S.Rees@bath.ac.uk

Syakila Ahmad
syakilaahmad@usm.my

1 School of Mathematical Sciences, Universiti Sains Malaysia, 11800 Penang, Malaysia

2 Department of Mechanical Engineering, University of Bath, Bath BA2 7AY, UK

p	Pressure
Ra	Darcy–Rayleigh number
T	Dimensional temperature
u	Horizontal velocity
w	Vertical velocity
x	Horizontal coordinate
z	Vertical coordinate

Greek symbols

α	Constant given in Eq. (57)
β	Expansion coefficient
γ_1, γ_2	Constants given in Eq. (43)
θ	Temperature
Θ	Disturbance temperature
κ	Thermal diffusivity
μ	Dynamic viscosity
ρ	Density
ψ	Streamfunction
Ψ	Disturbance streamfunction
Ω	Constant given in Eq. (46)

Subscripts and superscripts

c	Cold
h	Hot
i	Denoting sidelayers 1 or 2
1, 2	Sidelayer indices
$\hat{}$	Dimensional quantity
$'$	Derivative with respect to x

1 Introduction

The topic of convective flows in porous media is important because it is a ubiquitous process in the world around us and in many and varied technological applications. Of particular importance are those systems which display transitions in behaviour as the strength of heating is altered. For example, quiescent states (and others) may be destabilised and cellular patterns might be formed as heating increases, and generally these transitions also alter the rate of heat flux across the system, which may be either good or bad depending on the application.

The Darcy–Bénard problem is the classical thermoconvective instability problem for convection in porous media, the first papers on which first appeared over 60 years ago: Lapwood (1948) and Horton and Rogers (1945). These pioneering works have been extended in a huge variety of ways a few decades later; see, for example, Nield (1968), Holst and Aziz (1972), Palm et al. (1972), Straus (1974), Weidman and Kassoy (1986), Chelghoum et al. (1987), Aidun and Steen (1987), Caltagirone et al. (1987), Riley and Winters (1991) and Nygård and Tyvand (2010). These studies include the effects of different boundary conditions, of nonlinearities, of large Darcy–Rayleigh numbers compared with the onset value, of confinement, of

oscillatory convection. In all of these cases it is the 'pure' Darcy flow model with the Boussinesq approximation that has been used. Other authors have considered form drag, Brinkman effects, multiple diffusing species, vibration, inclination, local thermal nonequilibrium and non-Newtonian fluids. We refer the reader to the reviews by Rees (2000), Tyvand (2002) and Nield and Bejan (2013).

The present paper is motivated by the fact that almost all the studies which one might find in the literature are model problems in the sense that it will be very difficult to be able reproduce them in the laboratory. A simple instance of this might involve, say, a cubical cavity filled with porous medium which is heated from below, cooled from above and insulated on its four vertical sidewalls. Typically these boundary conditions are applied on what would be, in an experiment, the inner surface of the bounding container, rather than on its outer surface.

To date there have appeared only a few studies which consider the effect of solid bounding walls, and these are confined mainly to the upper and lower surfaces. Mojtabi and Rees (2011) considered Darcy–Bénard convection in a layer of infinite horizontal extent where the outer surfaces of the solid layers were subject to constant-heat-flux conditions. They found that, for certain ranges of parameters (i.e. conductivity ratios and the thickness of the solid layers) that it is possible for such a system to mimic quite closely that of the idealised classical Darcy–Bénard layer with constant temperature boundary conditions. Similar analyses were undertaken by Kubitschek and Weidman (2003, 2006). Much earlier, Riahi (1983) considered solid layers of infinite thickness and determined, using a weakly nonlinear theory, the region of parameter space wherein square cells are preferred as opposed to rolls when the Darcy–Rayleigh number is just supercritical. Both of these papers were extended by Rees and Mojtabi (2011) who undertook the constant-temperature-surface analogue of Mojtabi and Rees (2011) and also presented the corresponding weakly nonlinear theory.

In the present paper we consider the effect of solid, thermally conducting sidewalls on the onset of convection. Wang et al. (1987) provides the closest study to the present one, and it corresponds to an asymptotically thin vertical porous slab sandwiched between the solid blocks. The present analysis considers a porous cavity with $O(1)$ thickness, and we provide a comprehensive account of the onset of convection for the full range of values of the conductivity ratio between the porous medium and the block, the thickness of the block, and the width of the porous cavity. In addition, an asymptotic analysis is presented for small values of the parameter, Ω, which is a function of the conductivity ratio and the thickness of the block.

2 Governing Equations

We consider the onset of convection in a rectangular porous cavity which is heated from below. The height of this cavity is h and the length is hL, and therefore L represents the aspect ratio. Although the horizontal surfaces are assumed to be subject to uniform fixed temperatures, where the lower surface is held at $T = T_h$ and the upper at $T = T_c$, the sidewalls are shrouded using solid but thermally conducting sidelayers of thickness hd. The outside surfaces of both these side layers are either perfectly insulated or else are held at precisely that linear heat conduction profile which corresponds to the imposed upper and lower surface temperatures. These details are summarised in Fig. 1 where we note, in particular, that the conductivity of the porous medium is k while that of the two solid sidelayers is k_s. We will consider solely those cases where the sidelayers are identical.

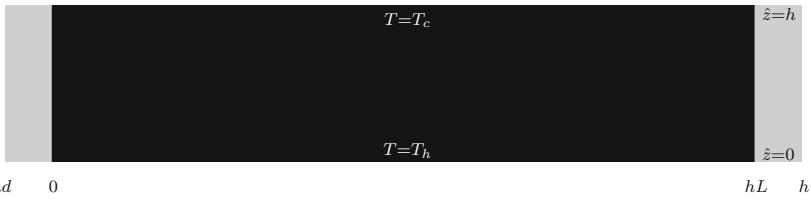

Fig. 1 The physical configuration consisting of a central porous layer (depicted in *black*) with two conducting solid sidelayers (*grey*). The left- and right-hand boundary conditions are either (i) a linear temperature profile as given by Eq. (10), or (ii) insulated

The conservation of mass corresponds to,

$$\frac{\partial \hat{u}}{\partial \hat{x}} + \frac{\partial \hat{w}}{\partial \hat{z}} = 0, \tag{1}$$

while Darcy's law for a Newtonian fluid (subject to the Boussinesq approximation being valid and a linear relationship between the density and temperature) takes the form,

$$\hat{u} = -\frac{K}{\mu}\frac{\partial \hat{p}}{\partial \hat{x}}, \tag{2}$$

$$\hat{w} = -\frac{K}{\mu}\left[\frac{\partial \hat{p}}{\partial \hat{z}} - \rho g \beta (T - T_c)\right]. \tag{3}$$

The steady heat transport equation for the porous region is given by,

$$\hat{u}\frac{\partial T}{\partial \hat{x}} + \hat{w}\frac{\partial T}{\partial \hat{z}} = \kappa\left[\frac{\partial^2 T}{\partial \hat{x}^2} + \frac{\partial^2 T}{\partial \hat{z}^2}\right]. \tag{4}$$

while for each of the two side layers it is,

$$\frac{\partial^2 T_i}{\partial \hat{x}^2} + \frac{\partial^2 T_i}{\partial \hat{z}^2} = 0, \tag{5}$$

where $i = 1$ denotes the left-hand side layer for which $-hd < \hat{x} < 0$, and $i = 2$ denotes the right-hand side layer for which $hL < \hat{x} < h(L + d)$. The boundary and interface conditions are given by

$$\hat{w} = 0, \qquad T = T_1 = T_2 = T_h \quad \text{on } \hat{z} = 0, \tag{6}$$

$$\hat{w} = 0, \qquad T = T_1 = T_2 = T_c \quad \text{on } \hat{z} = h, \tag{7}$$

while the outer vertical surfaces are subject to,

$$\text{case (a):} \quad \begin{aligned} &T_1 = T_c + (1 - z/h)(T_h - T_c) \quad \text{on } \hat{x} = -hd, \\ &T_2 = T_c + (1 - z/h)(T_h - T_c) \quad \text{on } \hat{x} = h(L + d), \end{aligned} \tag{8}$$

or

$$\text{case (b):} \quad \frac{\partial T_1}{\partial \hat{x}} = 0 \quad \text{on } \hat{x} = -hd, \qquad \frac{\partial T_2}{\partial \hat{x}} = 0 \quad \text{on } \hat{x} = h(L + d). \tag{9}$$

The conditions at the interfaces are,

$$\begin{aligned} &\hat{u} = 0, \quad T_1 = T, \quad k_s \frac{\partial T_1}{\partial \hat{x}} = k \frac{\partial T}{\partial \hat{x}} \quad \text{on } \hat{x} = -hd, \\ &\hat{u} = 0, \quad T_2 = T, \quad k_s \frac{\partial T_2}{\partial \hat{x}} = k \frac{\partial T}{\partial \hat{x}} \quad \text{on } \hat{x} = h(L+d). \end{aligned} \tag{10}$$

We may now create a set of nondimensional equations using the following scalings,

$$(\hat{x}, \hat{z}) = h(x, z), \qquad (\hat{u}, \hat{w}) = \frac{\kappa}{h}(u, w), \qquad T = T_c + \theta(T_h - T_c), \tag{11}$$

and define the streamfunction, ψ, using,

$$u = -\frac{\partial \psi}{\partial z}, \qquad w = \frac{\partial \psi}{\partial x}. \tag{12}$$

Thus the nondimensional governing equations and boundary/interface conditions become,

$$\frac{\partial^2 \psi}{\partial x^2} + \frac{\partial^2 \psi}{\partial z^2} = Ra \frac{\partial \theta}{\partial x}, \tag{13}$$

$$\frac{\partial \psi}{\partial x}\frac{\partial \theta}{\partial z} - \frac{\partial \psi}{\partial z}\frac{\partial \theta}{\partial x} = \frac{\partial^2 \theta}{\partial x^2} + \frac{\partial^2 \theta}{\partial z^2}, \tag{14}$$

$$\frac{\partial^2 \theta_i}{\partial x^2} + \frac{\partial^2 \theta_i}{\partial z^2} = 0, \qquad (i = 1, 2), \tag{15}$$

$$\psi = 0, \qquad \theta = \theta_1 = \theta_2 = 1 \quad \text{on } z = 0, \tag{16}$$

$$\psi = 0, \qquad \theta = \theta_1 = \theta_2 = 0 \quad \text{on } z = 1, \tag{17}$$

$$\text{case (a):} \quad \theta_1 = (1 - z) \quad \text{on } x = -d, \qquad \theta_2 = (1 - z) \quad \text{on } x = L + d, \tag{18}$$

or

$$\text{case (b):} \quad \frac{\partial \theta_1}{\partial x} = 0 \quad \text{on } x = -d, \qquad \frac{\partial \theta_2}{\partial x} = 0 \quad \text{on } x = L + d, \tag{19}$$

$$\begin{aligned} &\psi = 0, \quad \theta_1 = \theta, \quad c \frac{\partial \theta_1}{\partial x} = \frac{\partial \theta}{\partial x} \quad \text{on } x = -d, \\ &\psi = 0, \quad \theta_2 = \theta, \quad c \frac{\partial \theta_2}{\partial x} = \frac{\partial \theta}{\partial x} \quad \text{on } x = L + d. \end{aligned} \tag{20}$$

Here the value c is the conductivity ratio,

$$c = \frac{k_s}{k}, \tag{21}$$

and

$$Ra = \frac{\rho g \beta (T_h - T_c) K h}{\mu \kappa}, \tag{22}$$

is the Darcy–Rayleigh number. Thus, at this stage, solutions depend on four parameters: Ra, L, d and c.

3 Basic State and Stability Analysis

The basic state is given by,

$$\theta = \theta_1 = \theta_2 = 1 - z, \qquad \psi = 0, \tag{23}$$

and hence there is a linear temperature drop across the layer with no flow. We may perturb about this solution by setting,

$$\theta = 1 - z + \Theta, \quad \theta_1 = 1 - z + \Theta_1, \quad \theta_2 = 1 - z + \Theta_2, \quad \psi = \Psi. \tag{24}$$

Substitution of these expressions into Eqs. (13)–(20) followed by linearisation yields the systems,

$$\frac{\partial^2 \Psi}{\partial x^2} + \frac{\partial^2 \Psi}{\partial z^2} = Ra \frac{\partial \Theta}{\partial x}, \tag{25}$$

$$\frac{\partial^2 \Theta}{\partial x^2} + \frac{\partial^2 \Theta}{\partial z^2} = -\frac{\partial \Psi}{\partial x}, \tag{26}$$

$$\frac{\partial^2 \Theta_1}{\partial x^2} + \frac{\partial^2 \Theta_1}{\partial z^2} = 0, \tag{27}$$

$$\frac{\partial^2 \Theta_2}{\partial x^2} + \frac{\partial^2 \Theta_2}{\partial z^2} = 0. \tag{28}$$

The boundary conditions on the horizontal surfaces are that

$$\Psi = \Theta = \Theta_1 = \Theta_2 = 0 \quad \text{on } z = 0, 1, \tag{29}$$

while the outer vertical surfaces are subject to,

$$\text{case (a):} \quad \Theta_1 = 0 \quad \text{on } x = -d, \qquad \Theta_2 = 0 \quad \text{on } x = L + d, \tag{30}$$

or

$$\text{case (b):} \quad \frac{\partial \Theta_1}{\partial x} = 0 \quad \text{on } x = -d, \qquad \frac{\partial \Theta_2}{\partial x} = 0 \quad \text{on } x = L + d. \tag{31}$$

The conditions at the interfaces are,

$$\begin{aligned} &\Psi = 0, \quad \Theta_1 = \Theta, \quad c\frac{\partial \Theta_1}{\partial x} = \frac{\partial \Theta}{\partial x} \quad \text{on } x = 0, \\ &\Psi = 0, \quad \Theta_2 = \Theta, \quad c\frac{\partial \Theta_2}{\partial x} = \frac{\partial \Theta}{\partial x} \quad \text{on } x = L. \end{aligned} \tag{32}$$

When undertaking the linear stability analysis of a convecting system, it is very common to factor out a horizontal Fourier component which serves to impose a horizontal periodicity on the convecting pattern. In the present problem, though, we shall instead factor out a vertical component as follows. We let,

$$(\Psi, \Theta, \Theta_1, \Theta_2) = \Big(F(x), G(x), G_1(x), G_2(x)\Big) \sin \pi z. \tag{33}$$

This process yields an ordinary differential eigenvalue problem for Ra,

$$F'' - \pi^2 F = Ra\, G', \tag{34}$$

$$G'' - \pi^2 G = -F', \tag{35}$$

$$G_i'' - \pi^2 G_i = 0, \qquad (i = 1, 2) \tag{36}$$

where the boundary and interface conditions are,

$$\begin{aligned} x = -d: &\quad G_1 = 0 \quad \text{case (a)}, \quad G_1' = 0 \quad \text{case (b)}, \\ x = 0: &\quad G_1 = G, \quad cG_1' = G', \quad F = 0, \\ x = L: &\quad G_2 = G, \quad cG_2' = G', \quad F = 0, \\ x = L + d: &\quad G_2 = 0 \quad \text{case (a)}, \quad G_2' = 0 \quad \text{case (b)}. \end{aligned} \tag{37}$$

It is possible to solve for the disturbance field within the sidelayers and to convert this into an equivalent boundary condition for the porous region; see Kubitschek and Weidman (2003, 2006) and Mojtabi and Rees (2011) who present a similar technique to account for conducting layers above and below the cavity. The equation for G_1 in Eq. (36) and subject to the boundary condition at $x = -d$ has solution,

$$\begin{aligned} \text{case (a):} \quad G_1 &= A\Big[\sinh \pi x + \tanh \pi d \cosh \pi x\Big], \\ \text{case (b):} \quad G_1 &= A\Big[\sinh \pi x + \coth \pi d \cosh \pi x\Big], \end{aligned} \tag{38}$$

where A is an arbitrary constant. In each case we may evaluate G_1 and G_1' at $x = 0$ and eliminate A between these expressions to obtain the following boundary conditions of the third kind,

$$\text{case (a):} \quad \pi G_1 = \tanh \pi d \, G_1', \qquad \text{case (b):} \quad \pi G_1 = \coth \pi d \, G_1'. \tag{39}$$

Given the interface conditions shown in Eq. (37) the boundary conditions which may be applied at $x = 0$ for the porous layer and which account perfectly for the presence of the sidelayer are

$$\text{case (a):} \quad \pi G = \frac{\tanh \pi d}{c} G', \quad \text{case (b):} \quad \pi G = \frac{\coth \pi d}{c} G'. \tag{40}$$

The equivalent forms at $x = L$ may be shown easily to be,

$$\text{case (a):} \quad \pi G = -\frac{\tanh \pi d}{c} G', \quad \text{case (b):} \quad \pi G = -\frac{\coth \pi d}{c} G'. \tag{41}$$

Equations (34) and (35) may now be solved analytically subject to the conditions, $F(0) = F(L) = 0$ and those given in Eqs. (40) and (41). This involves the substitution of the trial solution, $e^{\gamma x}$, and imposing the requirement that the equations have a nonzero solution. This leads naturally to a dispersion relation for the Darcy–Rayleigh number, Ra, in terms of L and d. We eventually obtain the following expression,

$$\begin{aligned} 0 = {} & 2\pi^2 c^2 \Big(1 - \sin \gamma_1 L \, \sin \gamma_2 L - \cos \gamma_1 L \, \cos \gamma_2 L\Big) \\ & + 2\pi c(\gamma_1 - \gamma_2) \tanh \pi d \, \Big(\sin \gamma_2 L \, \cos \gamma_2 L - \sin \gamma_2 L \, \cos \gamma_1 L\Big) \\ & + (\gamma_1 - \gamma_2)^2 \tanh^2 \pi d \, \sin \gamma_1 L \, \sin \gamma_2 L, \end{aligned} \tag{42}$$

where the auxiliary quantities, γ_1 and γ_2, are given by,

$$\begin{aligned} {\gamma_1}^2 &= \frac{Ra}{2} - \pi^2 + \frac{\sqrt{Ra}}{2}\Big[Ra - 4\pi^2\Big]^{1/2}, \\ {\gamma_2}^2 &= \frac{Ra}{2} - \pi^2 - \frac{\sqrt{Ra}}{2}\Big[Ra - 4\pi^2\Big]^{1/2}. \end{aligned} \tag{43}$$

The dispersion relation in Eq. (42) corresponds to case (a) and the equivalent formula for case (b) may be obtained by replacing all the tanh functions by coth functions.

The form taken by the dispersion relation hints strongly that it might be possible to factorise it into the product of two factors, a process that is known to arise occasionally and other examples may be found in Rees and Genç (2010). Therefore we obtain the following pair of relations,

$$\pi c\Big(\sin\gamma_1 L\cos\gamma_2 L-\sin\gamma_2 L\cos\gamma_1 L+\sin\gamma_1 L-\sin\gamma_2 L\Big) +(\gamma_1-\gamma_2)\tanh\pi d\ \sin\gamma_1 L\ \sin\gamma_2 L=0, \tag{44}$$

$$\pi c\Big(\sin\gamma_1 L\cos\gamma_2 L-\sin\gamma_2 L\cos\gamma_1 L-\sin\gamma_1 L+\sin\gamma_2 L\Big) +(\gamma_1-\gamma_2)\tanh\pi d\ \sin\gamma_1 L\ \sin\gamma_2 L=0. \tag{45}$$

These different factors correspond respectively to the odd and even symmetries of the onset mode.

Given the forms of γ_1 and γ_2, it is impossible to write down the value of Ra explicitly as a function of the length, L, of the porous cavity, the conductivity ratio, c, and the width of the sidelayers, d. Therefore we have resorted to using either (i) a straightforward Newton–Raphson scheme to solve for Ra in terms of L, c and d, or (ii) creating a fine two-dimensional grid in terms of Ra and L of values of the function on the right-hand side of Eq. (42) and then using a contouring package to determine where this function is equal to zero; such a procedure is guaranteed to find all the branches of the neutral curves within the chosen range. Profiles for the onset modes were obtained using the detailed analysis (omitted here for the sake of brevity) leading to the dispersion relation, and were checked by solving Eqs. (34) and (35) subject to the boundary conditions (40) and (41) using a shooting method and the classical fourth order Runge–Kutta method.

4 Results and Discussion

We begin the presentation of the results of our analysis by noting that the dispersion relation given by Eq. (42) is a function of only three variables, namely, Ra, L and $(\tanh\pi d)/c$ for case (a) flows, rather than four: Ra, L, d and c. For case (b) flows precisely the same form of dispersion relation applies, and this is the *same* function of Ra, L and $(\coth\pi d)/c$. Given that both $(\tanh\pi d)/c$ and $(\coth\pi d)/c$ may range in value from zero to infinity when c and d take various physically realistic values, the two different problems we are solving and which are differentiated by having different sidelayer boundary conditions, may be unified into one problem. We may therefore define the quantity, Ω, according to

$$\text{case (a):}\quad \Omega=\frac{\tanh\pi d}{c},\qquad \text{case (b):}\quad \Omega=\frac{\coth\pi d}{c}. \tag{46}$$

Thus critical values of Ra will now depend only on the two parameters, Ω and L. We have validated our numerical scheme against that of Nygård and Tyvand (2010) for the case, $\Omega=\pi$ (which is equivalent to their case $a=1$ and $b=0$), with $L=1/2$ and $L=1$; our critical values are identical to theirs.

4.1 Disturbance Profiles

Figure 2 illustrates the effect on the onset profile of having different pairs of values of c and d which combine to yield $\Omega = 1$. The temperature profiles presented in Fig. 2 include those in both sidelayers. Given that $\Omega = 1$ the disturbance profile in the porous region is the same in each case, but the sections of profile which occupy the sidelayers depend strongly on the chosen value of d and whether the problem is case (a) or case (b). It is also clear that, as d increases, cases (a) and (b) tend to become indistinguishable from one another. This is simply the consequence of the exponential decay of the profile in the solid sidelayers. In the rest of the paper we will concentrate mainly on the effect of having different values of Ω without necessarily specifying whether case (a) or (b) is meant because either may apply.

Figures 3 and 4 show the effect of having different values of Ω on porous cavity with $L = 1$. We show those profiles which correspond to the smallest critical value of Ra, and they correspond to temperature profiles which are odd about $x = L/2$. Figure 3 displays the temperature disturbances, and Fig. 4 shows the corresponding streamfunction disturbances. The value, $\Omega = 10^4$, essentially corresponds to when the sidelayers are effectively insulating and therefore this case mimics the classical Darcy–Bénard problem in a unit box for which $Ra = 4\pi^2$. The disturbance temperature profile shown in Fig. 3 is then proportional to $\cos \pi x$, while the corresponding streamfunction profile in Fig. 4 is proportional to $\sin \pi x$.

As Ω decreases, the sidelayers increase their conductivity until one obtains the perfectly conducting limit, $\Omega = 0$. This limit was studied in detail in Rees and Tyvand (2004); also see Lyubimov (1975), Nilsen and Storesletten (1990), Bratsun et al. (1995) and Rees and Lage (1997). For the unit box the critical Darcy–Rayleigh number is $8\pi^2$, therefore a perfectly conducting sidelayer inhibits convection relative to a perfectly insulating sidelayer.

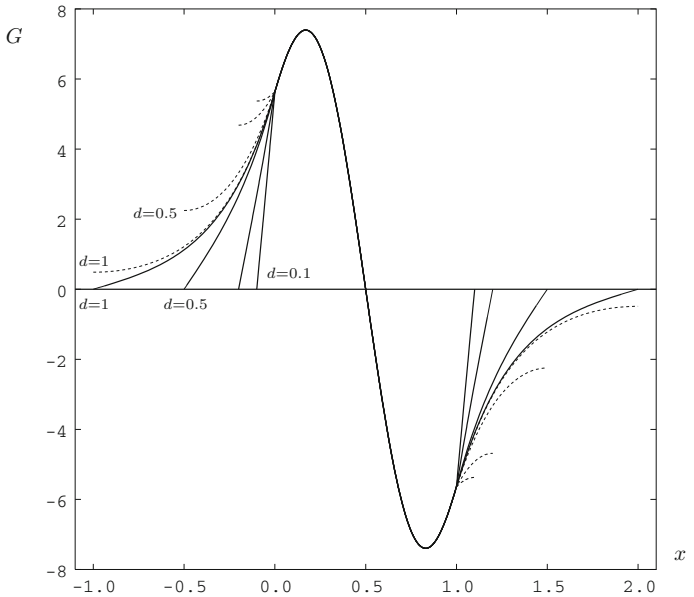

Fig. 2 Displaying the temperature disturbance profile when $\Omega = 1$ and $L = 1$. *Continuous lines* correspond to case (a), while *dashed lines* correspond to case (b). The following values of d were used: 0.1, 0.2, 0.5 and 1.0. The critical Darcy–Rayleigh number is $Ra = 56.96696$

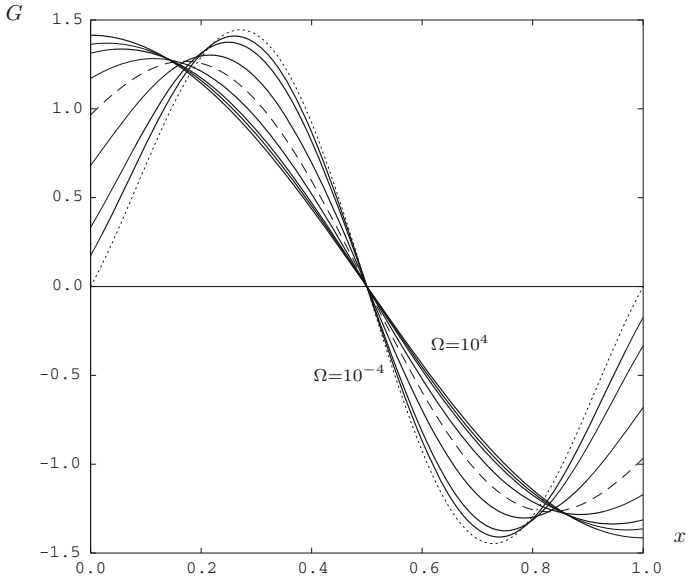

Fig. 3 Displaying the temperature disturbance profile in the porous region for the case, $L = 1$, and for different values of Ω: 10^4, 10, 5, 2, 1 (*long dashes*), 0.5, 0.2, 0.1 and 10^{-4} (*dotted*)

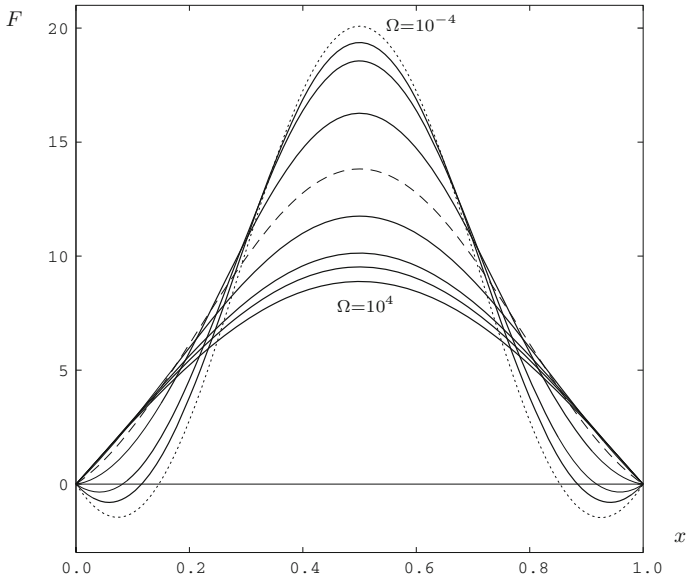

Fig. 4 Displaying the streamfunction disturbance profile in the porous region for the case, $L = 1$, and for different values of Ω: 10^4, 10, 5, 2, 1 (*long dashes*), 0.5, 0.2, 0.1 and 10^{-4} (*dotted*)

The corresponding temperature and streamfunction profiles may gleaned from the analysis of Rees and Tyvand (2004) and are,

$$G \propto \sin \pi x \, \cos \sqrt{2}\pi \left(x - \tfrac{1}{2}\right), \qquad F \propto \sin \pi x \, \sin \sqrt{2}\pi \left(x - \tfrac{1}{2}\right). \tag{47}$$

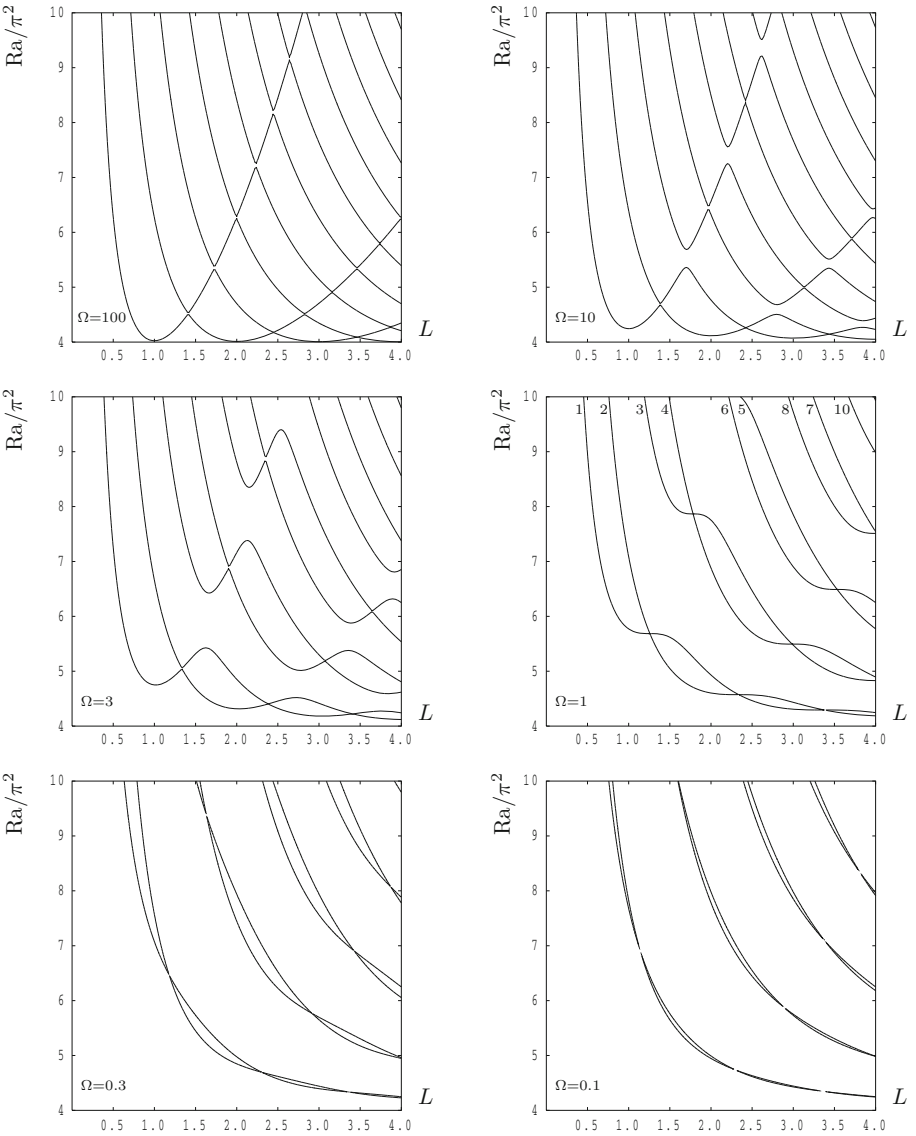

Fig. 5 Displaying neutral curves (*Ra* against *L*) for different values of Ω

We note that these solutions in (47) are also displayed in the form of full two-dimensional contour plots in Fig. 1a of Rees and Tyvand (2004).

4.2 Neutral Curves

Figure 5 displays six sets of neutral curves corresponding, respectively, to $\Omega = 100$, 10, 3, 1, 0.3 and 0.1. These were obtained using the aforementioned contouring procedure and display the variation of Ra/π^2 with L.

When Ω is sufficiently large we recover the behaviour one expects for insulated boundaries. The neutral curves are given by,

$$Ra = \frac{(L^2 + n^2)^2}{n^2 L^2}\pi^2, \tag{48}$$

where n is the number of convection cells in the horizontal direction (i.e. the number of half sine waves comprising the reduced streamfunction, F). The value of Ra achieves its minimum value of $4\pi^2$ whenever $L = n$. For this extreme case it is easy to identify the different modes with the value of n, and we see that, as L increases from zero, successive values of n starting from 1 take over briefly as the mode which has the smallest value of Ra. Thus one would normally identify the mode number with a single parabolic-like curve of the type approximated in the subfigure showing $\Omega = 100$. However, once Ω takes finite values, the shapes of the neutral curves change and curves corresponding to two different odd modes, say, no longer cross one another but these crossings unfold. Therefore it is necessary to use a different modal numbering system, as illustrated in the subfigure for $\Omega = 1$. In general, then, when Ω takes finite values, neutral curves are split into pairs consisting of one odd mode and one even mode, where respective members of each pair intertwine thereby continually swapping roles as the one with the lower value of Ra as L increases. From the point of view of determining the smallest value of Ra, the intertwining of the first two modes ensures that odd and even modes (in terms of both their mode number and the symmetry of the disturbance temperature profile) alternate as the primary mode of instability.

As Ω finally reduces towards zero, Fig. 5 shows that the neutral curves for modes 1 and 2 get closer and tend towards a common limit when $\Omega = 0$. This is perfectly consistent with the analysis of Rees and Tyvand (2004) who described a degenerate onset of convection in which two different modes correspond to precisely the same value of the critical Darcy–Rayleigh number. Rees and Tyvand (2004) showed that the critical Darcy–Rayleigh number for the perfectly conducting case is

$$Ra = 4\pi^2\left(1 + \frac{1}{L^2}\right), \tag{49}$$

in the present notation. It is also important to note that the small gaps in neutral curves which appear for the cases, $\Omega = 0.3$ and 0.1 in Fig. 5 are simply an artefact of the grid resolution used for the contour plotter which employed the dispersion relation in Eq. (42); the curves are continuous in reality. Indeed, "Appendix 1" provides a detailed mathematical analysis of the onset criterion for small values of Ω, and it is clear from Eq. (64) that the odd and even modes interleave as L increases, with the largest gap between these curves decreasing as L^{-3}.

From Fig. 5 it also appears that the critical value of Ra decreases monotonically as L increases when Ω is less than a value which is very close to 1.

Given that the most important value of Ra is the lowest for any chosen value of Ω and L, we have summarised these minimising values in Fig. 6 and have also indicated whether the mode is even or odd. Thus, for small values of L, we see that the onset mode is odd, and further increases in L cause the symmetry to alternate successively between odd and even. Also shown there as dotted lines are the curves in (L, Ra)-space which delineate where the modal exchange takes place. These were obtained using a slightly more complicated Newton–Raphson procedure where the factored dispersion relations which are given in Eqs. (44) and (45) are solved simultaneously while insisting that they have identical values of Ra. For a given value of Ω this process yields the values of both Ra and L.

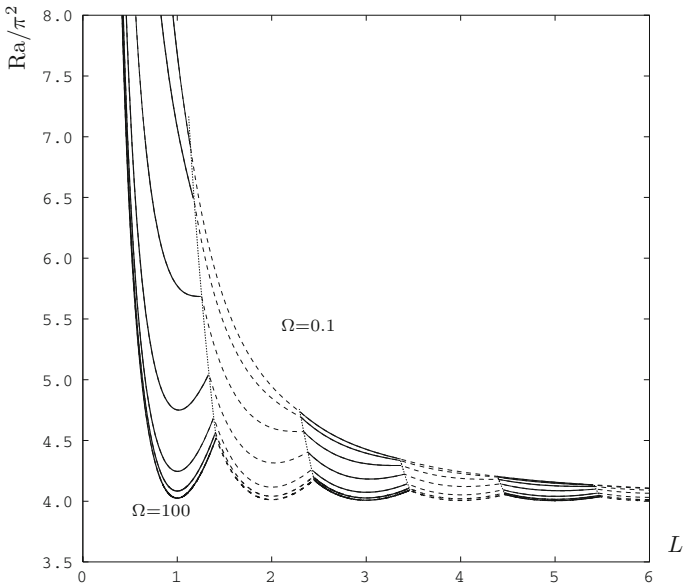

Fig. 6 Variation of *Ra* with L corresponding to the primary mode of instability for the following values of Ω: 100 (*lowest curve*), 30, 10, 3, 1, 0.3 and 0.1 (*uppermost curve*). *Continuous lines* correspond to odd temperature disturbances, while *dashed lines* correspond to even disturbances. The *dotted lines* delineate the transition between odd and even modes

5 Conclusions

In this paper we have relaxed the classical Darcy–Bénard problem by allowing the insulating sidewalls of the rectangular porous cavity to be replaced by sidelayers of thermally conducting solid material. The outer vertical boundaries of these sidelayers may be considered to be either perfectly insulating or perfectly conducting, but the form of the dispersion relation we have obtained shows that both may be subsumed into one unified form involving the parameter, Ω. In general, as the aspect ratio of the porous cavity, L, increases, the identity of the most unstable mode alternates between one with a temperature profile which is odd (which arises when $L \ll 1$) and one which is even. In general the critical Darcy–Rayleigh number decreases with L, but it does so monotonically only when $\Omega \lesssim 1$.

This paper forms an extension to the standard Darcy–Bénard problem since it is concerned with the additional effect of conducting layers on the sidewalls of a rectangular Darcy–Bénard cavity. We have seen that their effect is strong and the stability properties have been shown to vary continuously between that of the classical Darcy–Bénard problem and that of the degenerate system studied recently by Rees and Tyvand (2004). A similar analysis by Mojtabi and Rees (2011) considered the use of conducting plates above and below the Darcy–Bénard cell; in that paper it was shown the stability properties also vary greatly and that the full range of cases between the classical Darcy–Bénard system and its constant-heat-flux analogue may be realised. It may therefore be thought that these two studies may be combined easily into one where conducting plates might be situated along all four sides of a rectangular cavity, which would represent even more fully an experimental set-up. While this is perfectly reasonable notion, the basic state whose stability properties are to be studied will not, in general, consist of horizontal isotherms and therefore there is also a localised flow field near the four corners

of the cavity. An isolated exception to this is when the conductivities of the porous layer and the side layers are identical, although even that depends on precisely how one joins the sidelayers to the upper and lower layers. Thus a full stability analysis will involve numerical solutions of a fully elliptic partial differential eigenvalue problem.

The present paper has considered the experimentally reasonable configuration in which the conducting sidelayers are identical. We have found that the neutral curves bunch in pairs, the two members of which correspond to different symmetries. If the two sidelayers were to be different, then these precise symmetries would be lost. We suspect that the curves within each pair would unfold, so that there would no longer be such crossings, and, in particular, the lowest neutral curve would be smooth. This prediction would need to be tested numerically.

Finally, the present analysis represents the first stage in a full understanding of the effect of conducting sidewalls. It will be necessary to consider the onset of convection in the form of vortices which have axes in the x-direction. It is intended to report on this aspect in due course.

Acknowledgments The first author would like to thank the Universiti Sains Malaysia for providing funding and support for her stay at the University of Bath. The authors wish to thank the reviewers for their kind remarks and suggestions. We are especially grateful for one particular observation the consequence of which is outlined in "Appendix 2".

Appendix 1

The aim of this appendix is to provide a two-term analysis of the onset criterion for asymptotically small values of Ω in order (i) to determine the detailed approach to the degenerate criterion described in Rees and Tyvand (2004) in which two different modes become unstable simultaneously, and (ii) to explaining the braiding of the neutral curves shown in Fig. 5.

We begin with Eqs. (34) and (35), which are reproduced below for the sake of completeness,

$$F'' - \pi^2 F = Ra\, G', \qquad G'' - \pi^2 G = -F', \tag{50}$$

and the boundary conditions given by Eqs. (37), (40) and (41) as simplified/unified using Eq. (46), and which may be written in the form,

$$x = 0: \quad F = 0,\ G = \Omega G'/\pi, \qquad x = L: \quad F = 0,\ G = -\Omega G'/\pi. \tag{51}$$

The following analysis for $\Omega \ll 1$ is facilitated by a minor coordinate change in order that the porous layer lies between $-L/2$ and $+L/2$, rather than between 0 and L.

The following series expansion for small values of Ω may now be introduced,

$$\begin{aligned} F &= F_0(x) + \Omega F_1(x) + O(\Omega^2), \\ G &= G_0(x) + \Omega G_1(x) + O(\Omega^2), \\ Ra &= Ra_0 + \Omega Ra_1 + O(\Omega^2). \end{aligned} \tag{52}$$

The equations and boundary conditions for F_0 and G_0 are given by

$$F_0'' - \pi^2 F_0 - Ra_0\, G_0' = 0, \qquad G_0'' - \pi^2 G_0 + F_0' = 0, \tag{53}$$

and

$$F_0 = G_0 = 0 \quad \text{at} \quad x = \pm L/2. \tag{54}$$

Our numerical solutions result in modes which are either even or odd, as given by the symmetry of the temperature disturbance. For the even mode, the analytical solution given in Rees and Tyvand (2004) may be written in the form,

$$F_0 = 2\pi\alpha \cos\frac{\pi x}{L} \sin\alpha\pi x, \qquad G_0 = \cos\frac{\pi x}{L} \cos\alpha\pi x, \tag{55}$$

for which,

$$Ra_0 = 4\pi^2\Big(1 + \frac{1}{L^2}\Big) \equiv 4\pi^2\alpha^2, \tag{56}$$

and where the constant, α, which is introduced for mathematical convenience, is given by,

$$\alpha = \sqrt{1 + \frac{1}{L^2}}. \tag{57}$$

For the odd mode the corresponding solution is

$$F_0 = -2\pi\alpha \cos\frac{\pi x}{L} \cos\alpha\pi x, \qquad G_0 = \cos\frac{\pi x}{L} \sin\alpha\pi x, \tag{58}$$

The equations and boundary conditions for F_1 and G_1 are given by

$$F_1'' - \pi^2 F_1 - Ra_0\, G_1' = Ra_1\, G_0', \qquad G_1'' - \pi^2 G_1 + F_1' = 0, \tag{59}$$

and

$$x = -L/2: \quad F_1 = 0, \quad G_1 = G_0', \qquad x = L/2: \quad F_1 = 0, \quad G_1 = -G_0'. \tag{60}$$

It is not necessary to solve these equations for F_1 and G_1 since our focus is on the value of Ra_1, which may be found by applying a standard solvability (or orthogonality) condition. In the present context this is obtained by multiplying the equation for F_1 by F_0 and the equation for G_1 by $Ra_0\, G_0$, adding the two, and then integrating that sum over the range $x = -\frac{1}{2}L$ to $x = \frac{1}{2}L$. Thus we have,

$$\begin{aligned}&\int_{-L/2}^{L/2}\Big[\Big(F_1'' - \pi^2 F_1 - Ra_0\, G_1'\Big)F_0 + \Big(G_1'' - \pi^2 G_1 + F_1'\Big)Ra_0 G_0\Big]\, dx \\ &= Ra_1 \int_{-L/2}^{L/2} F_0 G_0'\, dx.\end{aligned} \tag{61}$$

After some integrations by parts, the use of Eq. (53) to simplify most of the resulting integrals, it is possible to show that,

$$Ra_1 \int_{-L/2}^{L/2} F_0 G_0'\, dx = \frac{Ra_0}{\pi}\Big[\Big(G_0'(-L/2)\Big)^2 + \Big(G_0'(L/2)\Big)^2\Big]. \tag{62}$$

Detailed integrations yield,

$$\text{even mode:} \quad Ra_1 = -\frac{16\pi}{L^3}\cos^2\Big(\frac{\alpha\pi L}{2}\Big), \qquad \text{odd mode:} \quad Ra_1 = -\frac{16\pi}{L^3}\sin^2\Big(\frac{\alpha\pi L}{2}\Big). \tag{63}$$

Table 1 Comparison between numerical and asymptotic values of L for which the Ra_1 values coincide for even and odd modes

Ω	1st	2nd	5th
0	1.11807240	2.29128785	5.40832691
0.01	1.12056102	2.29189265	5.40843564
0.02	1.12304964	2.29249444	5.40854416
0.04	1.12791458	2.29368901	5.40877062
0.08	1.13721501	2.29604210	5.40919113

The asymptotic data using Eq. (66) are designated by $\Omega = 0$ here. Data are shown for the first, second and fifth crossings of the neutral curves

Therefore the first two terms in the small-Ω series for the critical Darcy–Rayleigh number are,

$$\begin{aligned} \text{even mode:} \quad Ra &= 4\pi^2\alpha^2 - \Omega\left[\frac{16\pi}{L^3}\cos^2\left(\frac{\alpha\pi L}{2}\right)\right] + O(\Omega^2), \\ \text{odd mode:} \quad Ra &= 4\pi^2\alpha^2 - \Omega\left[\frac{16\pi}{L^3}\sin^2\left(\frac{\alpha\pi L}{2}\right)\right] + O(\Omega^2). \end{aligned} \tag{64}$$

Thus small values of Ω serve to destabilise the system compared with that of the degenerate problem of Rees and Tyvand (2004). The presence of $\sin^2$ and $\cos^2$ in the $O(\Omega)$ terms means that the even and odd modes will alternate with regard to which one has the lower critical value of Ra. More precisely, we may identify those values of L for which the two modes have precisely the same value of Ra_1. This takes place when

$$\frac{\alpha\pi L}{2} = \pi/4, 3\pi/4, 5\pi/4, \ldots. \tag{65}$$

In other words, we have

$$L = \sqrt{\frac{n^2}{4} - 1}, \quad n = 3, 5, 7, \ldots. \tag{66}$$

This formula compares very well indeed with our numerical computations, as seen in Table 1. Indeed, we have also displayed the numerical results for a number of values of Ω which show that the application of Richardson's extrapolation technique confirms the $O(\Omega)$ nature of the numerical solutions, and the $\Omega \to 0$ limit itself. Indeed, a first extrapolation using the data for $\Omega = 0.01$ and 0.02 yields a prediction for the $\Omega = 0$ solution which has an absolute error of a magnitude of roughly 10^{-6}.

Appendix 2

We are grateful to an anonymous reviewer for pointing out that it is possible for the problem we have presented here to have a mathematically identical dual. This is based on the degeneracy explored in detail by Rees and Tyvand (2004) who considered convection in a rectangular porous cavity with perfectly conducting sidewalls. It was shown there that the streamfunction field and the temperature field satisfies identical equations and boundary conditions when written in the correct way. Given that the streamfunction and temperature must have different

symmetries, the implication then was that two separate solutions for (Ψ, Θ) with opposing symmetries corresponds to each value of the critical Rayleigh number. This is the degeneracy.

Aspects of the analysis of Rees and Tyvand (2004) may be extended easily to the present problem. One may consider an entirely equivalent problem where the sidelayers are perfectly conducting but are now permeable. This new perfectly conducting boundary is equivalent to the present impermeable boundary condition on the sides of the porous medium. A zero value of the streamfunction on the outer boundaries of the sidelayers in this dual configuration will be equivalent to the present perfectly conducting ones for the temperature, while a zero gradient of the streamfunction (which is equivalent to a further external passive reservoir of fluid) would be equivalent to the present insulating case. Although it is difficult to visualise how this latter might be set up in practice, it is nevertheless mathematically possible. Finally a trivial rescaling of the present streamfunction with respect to Ra followed by the swapping of the present Ψ and Θ will yield the dual problem which we have described, and Ω will now be defined in terms of a permeability ratio instead of a conductivity ratio. Therefore the dual problem will have identical neutral curves to those presented here.

References

Aidun, C.K., Steen, P.H.: Transition of oscillatory convective heat transfer in a fluid-saturated porous medium. AIAA J. Thermophys. Heat Transf. **1**, 268–273 (1987)

Bratsun, D.A., Lyubimov, D.V., Roux, B.: Co-symmetry breakdown in problems of thermal convection in porous medium. Phys. D **82**, 398–417 (1995)

Caltagirone, J.P., Fabrie, P., Combarnous, M.: De la convection naturelle oscillante en milieux poreux au chaos temporel. C. R. Acad. Sci. Paris II **305**, 549–553 (1987)

Chelghoum, D.E., Weidmann, P.D., Kassoy, D.R.: The effect of slab width on the stability of natural convection in confined saturated porous media. Phys. Fluids **30**, 1941–1947 (1987)

Holst, P.H., Aziz, K.: Transient three-dimensional natural convection in confined porous media. Int. J. Heat Mass Transf. **15**, 73–90 (1972)

Horton, C.W., Rogers Jr, F.T.: Convection currents in a porous medium. J. Appl. Phys. **16**, 367–370 (1945)

Kubitschek, J.P., Weidman, P.D.: Stability of a fluid-saturated porous medium heated from below by forced convection. Int. J. Heat Mass Transf. **46**, 3697–3705 (2003)

Kubitschek, J.P., Weidman, P.D.: Stability of a fluid-saturated porous medium contained in a vertical cylinder heated from below by forced convection. Heat Mass Transf. **42**, 789–794 (2006)

Lapwood, E.R.: Convection of a fluid in a porous medium. Proc. Camb. Philos. Soc. **4**, 508–521 (1948)

Lyubimov, D.V.: Convective motions in a porous medium heated from below. J. Appl. Mech. Tech. Phys. **16**, 257–261 (1975)

Mojtabi, A., Rees, D.A.S.: The onset of the convection in Horton–Rogers–Lapwood experiments: the effect of conducting bounding plates. Int. J. Heat Mass Transf. **54**(3), 293–301 (2011)

Nield, D.A.: Onset of thermohaline convection in a porous medium. Water Resour. Res. **11**, 553–560 (1968)

Nield, D.A., Bejan, A.: Convection in Porous Media, 4th edn. Springer, New York (2013)

Nilsen, T., Storesletten, L.: An analytical study on natural-convection in isotropic and anisotropic porous channels. Trans. A.S.M.E. J. Heat Transf. **112**, 396–401 (1990)

Nygård, H.S., Tyvand, P.A.: Onset of convection in a porous box with partly conducting and partly penetrative sidewalls. Transp. Porous Media **84**, 55–73 (2010)

Palm, E., Weber, J.E., Kvernvold, O.: On steady convection in a porous medium. J. Fluid Mech. **54**, 153–161 (1972)

Rees, D.A.S.: The stability of Darcy–Bénard convection. In: Vafai, K. (ed.) Handbook of Porous Media, pp. 521–558. Marcel Dekker, New York (2000)

Rees, D.A.S., Genç, G.: The onset of convection in porous layers with multiple horizontal partitions. Int. J. Heat Mass Transf. **54**, 3081–3089 (2010)

Rees, D.A.S., Lage, J.L.: The effect of thermal stratification on natural convection in a vertical porous insulation layer. Int. J. Heat Mass Transf. **40**, 111–121 (1997)

Rees, D.A.S., Mojtabi, A.: The effect of conducting boundaries on weakly nonlinear Darcy–Bénard convection. Transp. Porous Media **88**, 45–63 (2011)

Rees, D.A.S., Tyvand, P.A.: The Helmholtz equation for convection in two-dimensional porous cavities with conducting boundaries. J. Eng. Math. **49**, 181–193 (2004)
Riahi, D.N.: Nonlinear convection in a porous layer with finite conducting boundaries. J. Fluid Mech. **129**, 153–171 (1983)
Riley, D.S., Winters, K.H.: Time-periodic convection in porous media: the evolution of Hopf bifurcations with aspect ratio. J. Fluid Mech. **223**, 477–474 (1991)
Straus, J.M.: Large amplitude convection in porous media. J. Fluid Mech. **64**, 51–63 (1974)
Tyvand, P.A.: Onset of Rayleigh–Bénard convection in porous bodies. In: Ingham, D.B., Pop, I. (eds.) Transport Phenomena in Porous Media II, chap. 4. Pergamon, Oxford (2002)
Wang, M., Kassoy, D.R., Weidman, P.D.: Onset of convection in a vertical slab of saturated porous media between two impermeable conducting blocks. Int. J. Heat Mass Transf. **30**(7), 1331–1341 (1987)
Weidman, P.D., Kassoy, D.R.: The influence of side wall heat-transfer on convection in a confined saturated porous-medium. Phys. Fluids **29**, 349–355 (1986)